

***Plate-forme robotisée et automatisée pour la caractérisation microonde
par sonde coaxiale évanescente en milieu liquide***

***Nanorobotics and automated platform for microwave characterization
of liquids using coaxial evanescent probe***

Ronan Petit, Mohamed Sebbache and Kamel Haddadi

*Univ. Lille, CNRS, Centrale Lille, Univ. Polytechnique Hauts-de-France, UMR 8520 - IEMN - Institut
d'Électronique de Microélectronique et de Nanotechnologie, F-59000 Lille, France
Centre National de la Recherche Scientifique (CNRS), Université Lille, USR 3380 - IRCICA, Lille, France*

[*kamel.haddadi@univ-lille.fr*](mailto:kamel.haddadi@univ-lille.fr)

*Mots clés: Microondes, caractérisation diélectrique de liquides, permittivité complexe, nano-robotique
Index Terms: Microwaves, dielectric characterization, complex permittivity, nanorobotics*

Résumé/Abstract

Une plate-forme de caractérisation microonde en milieu liquide est proposée. Des sondes de mesure coaxiales exploitant le champ-proche évanescent sont conçues et réalisées afin de pallier le manque de résolution spatiale des sondes coaxiales ouvertes traditionnelles. Le liquide sous test est positionné sur un système de déplacement XYZ présentant une résolution de déplacement nanométrique. La solution proposée permet d'envisager des applications d'imagerie diélectrique quantitative dans la bande de fréquences 100 kHz – 53 GHz. Les premiers résultats de caractérisation en milieu liquide dans une configuration approche-retrait sont présentés et démontrent la viabilité de la solution proposée.

A measurement platform for microwave characterization of liquids is presented. Coaxial probes using evanescent near-fields are designed and realized to mitigate the lack of spatial resolution of conventional open-ended coaxial probes. The liquid under test is placed on a XYZ piezo-based positioning stage with nanometer displacement resolution. The proposed solution is a viable candidate to address quantitative dielectric imaging in the frequency range 100 kHz to 53 GHz. The experimental preliminary results considering characterization of liquid droplets using an approach-retract configuration are presented and demonstrate the viability of the approach proposed.

1 Introduction

Since the 1980s, coaxial probing structures have attracted the attention from the research community to address dielectric characterization of solid, liquid and biological materials [1]. The measurement system consists of an open-ended coaxial probe connected to a vector network analyzer (VNA) through a coaxial cable. The probe is in contact with a planar dielectric sample or immersed in a liquid. The material under test must be homogeneous within a volume sufficiently large to simulate a slab which is electrically infinite in size [2]. Measurement errors are attributed to air gaps between the coaxial probe and solid samples if they are not flat enough. Consequently, applications have been mainly oriented towards the characterization of liquids as the probe is immersed in the liquid sample [3]-[8]. Keysight Technologies® has introduced the *Dielectric Probe kit* that gathers probes, calibration kit and dedicated software for permittivity extraction from the measured complex reflection coefficient [9]. This solution needs a minimum volume under test of 15.7 mm³ that is mainly limited by the coaxial probe geometry. As emergent applications are related to dielectric characterization of relatively small volume of liquids, microwave near-field microscopy techniques have been introduced to reach resolution down to tens of nanometers, mainly determined by probe apex geometry [10]-[13].

The solution proposed in this paper is a compromise between open-ended coaxial probes and microwave near-field microscopy tools. We have designed and fabricated open coaxial transmission lines with tapered inner conductor and clear from outer conductor. The theoretical lateral resolution determined by the probe apex geometry is between 0.6 and 120 μm . As the measured complex reflection coefficient of the probe immersed in the liquid is function of the part of the tapered section in the liquid, a piezo-based nanorobotics XYZ scanning stage is used to control accurately the positioning of the probe tip in the liquid sample. To achieve high measurement repeatability due to movement of the coaxial cable during scanning operation, the microwave part including the VNA, the coaxial cable and probe are fixed and only the sample placed on the XYZ stage is moved under the probe tip.

In Section 2, electromagnetic simulations based on Ansys® CST and considering conventional and proposed probe structures are proposed to situate the improvement in terms of spatial resolution. The Section is completed with probe fabrication. In Section 3, the measurement platform including specifications is described. Experimental demonstrations using droplets of water are presented in Section 4 to validate the approach proposed at test frequencies 1 and 2 GHz.

2 Evanescent coaxial probe simulation and fabrication

The evanescent coaxial probes are made of commercial tungsten needles commonly used for DC probing. The needles are cut to a length of 2 cm length and connected to the aperture of a female SMA coaxial transition using Silver glue (Figure 1). The protruding section of the probe from the coaxial aperture has a length of 15 mm. The needle tip has an apex size of 120 μm . For information, needles with different diameters down to 0.6 μm have been purchased for future complementary studies. The simplicity of the proposed solution is relevant for the development of low cost dielectric characterization tools. In the following, electromagnetic simulations (Ansys® CST) considering conventional probe (diameter = 1 mm) and an evanescent probe (apex = 120 μm) are described (Figure 1). The dielectric material between inner and outer conductors is Polytetrafluoroethylene (PTFE) with relative dielectric constant 2.1 and considered lossless for both cases.

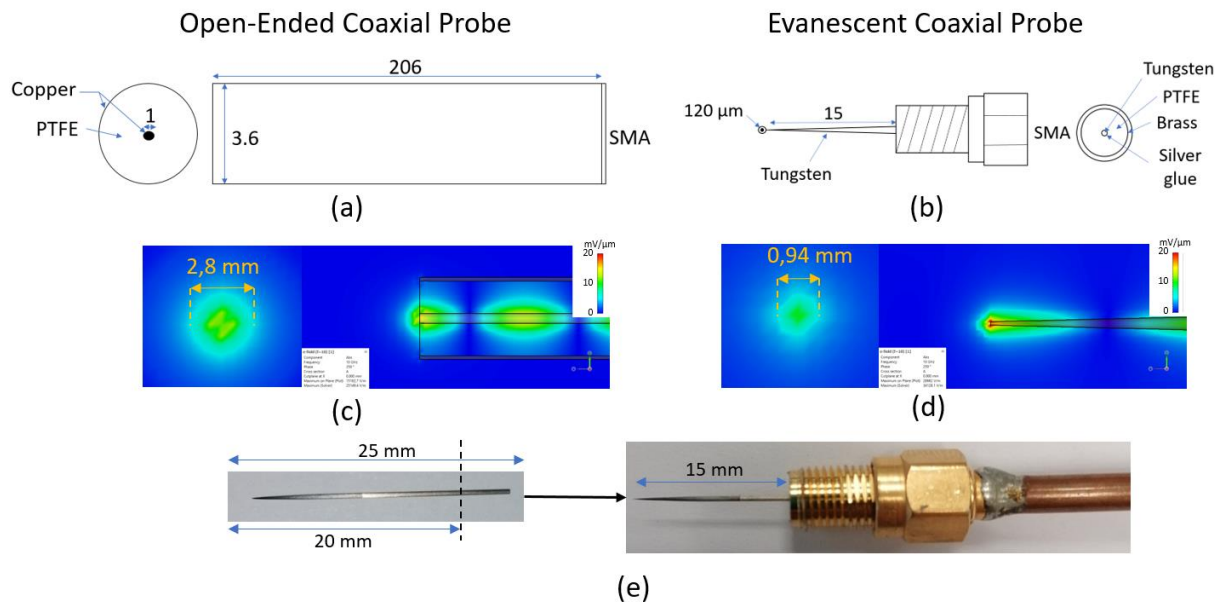


Figure 1. Geometry and dimensions of (a) open-ended coaxial probe and (b) proposed coaxial evanescent probe. Simulations of the microwave electric field distributions at the ISM frequency 2.45 GHz (Ansys® CST) considering (c) open-ended coaxial probe and (d) coaxial evanescent probe. (e) Assembly of the coaxial evanescent probe.

The electromagnetic simulations demonstrate a better collimating of the electric fields in the vicinity of the coaxial evanescent probe. In addition, the lateral resolution, that corresponds to the footprint of the electrical fields at the tip of the probe is improved by a ratio of approximatively 3. The electrical field reaches maximum value around 20 mV/ μm at the probe tip. Complementary electromagnetic simulations (not shown here) demonstrate that the electrical field decays exponentially as the distance to the probe increases. Consequently, the volume of the sample under test can be reduced to a volume that intercepts the electrical fields. In addition, dielectric imaging with high

spatial resolution can be addressed to address characterization of biological materials. The future works will include the impact of the apex size on both lateral and depth resolution that are two competitive parameters.

Accurate liquid characterization requires a fine control of the position of the probe tip in the liquid. Indeed, only one part of the needle is immersed in the liquid. The electric fields are distributed along the needle line both in the liquid and out of the liquid. The distribution of the electric fields contributes to the overall measured complex reflection coefficient. Consequently, a dedicated positioning platform based on nanorobotics is proposed in the next section to achieve accurate and repeatable measurements.

3 Nanorobotics microwave platform for liquid sensing applications

The nanorobotics microwave platform consists of two main components, a sample scanning stage and a dedicated microwave instrumentation. The sample scanning stage is composed of three piezo driven linear actuators manufactured by Smaract® GmbH with scanning ranges of 16mm in X and Y directions and 21mm in Z direction (see Table 1 for specifications) [14]-[15]. The XYZ positions are controlled in close-loop operation with nanometer resolution and ± 30 nm repeatability. The justification of using nanopositioning stages is related to future objectives to detect fine complex permittivity contrasts inside biological materials using smaller tip apex (0.6 μ m). These future applications, beyond the scope of this study, will require a well-controlled environment in terms of temperature, moisture content or mechanical vibrations. The RF probing unit consists of a coaxial evanescent probe connected to a coaxial cable itself connected to a VNA (P5008A Streamline Series USB VNA – Keysight Technologies®) through a semi-rigid coaxial cable. The input RF power and the intermediate frequency bandwidth (IFBW) are set to 0 dBm and 100 Hz respectively. The probe is positioned vertically over the stage and the material / liquid under test is moved under the probe thanks to the XYZ piezoelectric nano-positioning platform.

SmarAct® Reference	SLC2430	SLC1730
Axis	XY	Z
Travel [mm]	16	21
Dimensions [mm] [L x W x H]	30 x 24 x 10.5	30 x 17 x 8.5
Weight [g]	36	20
Resolution Open-Loop	< 1 [nm]	< 1 [nm]
Resolution Closed-Loop	1 (S) 4 (L) [nm]	1 (S) 4 (L) [nm]
Repeatability [nm]	± 30 (S) ± 60 (L)	± 30 (S) ± 60 (L)

Table 1. Nano-positioning XYZ stages specifications (Smaract® GmbH)

A camera is used for large-area visualization of the probe tip and the sample under test. Concerning the software part of the platform, a National Instruments LabVIEW® interface is developed to control the position of the sample, to set the network analyzer parameters, to record the resulting complex reflection coefficient S_{11} measured by the VNA and to display the results. (Figure 2).

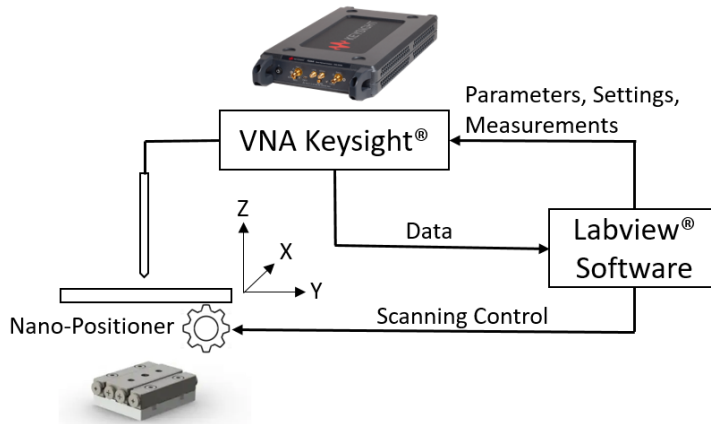


Figure 2. General overview of the proposed Nanorobotics microwave platform for liquid sensing applications.

The practical penetration depth limit is set by the instrument sensitivity and the probe geometry. Thus, the sensitivity of the reflection coefficient to the probe-to-object separation d has been first investigated. To that end, a planar metallic fixture (aluminum $S_{11} = -1$) is moved from the contact with the probe ($h=0$) to the distance $h=1000\mu\text{m}$ (step = $20\mu\text{m}$). All measurements are done at room temperature around 20°C . Figure 3 presents the distance dependence of the amplitude $|S_{11}|$ and phase-shift Φ_{11} of the reflection coefficient S_{11} . Experiments are performed at 1GHz and 2GHz respectively. Measurements are performed in both directions (attract and retract) to study the repeatability of the measurements.

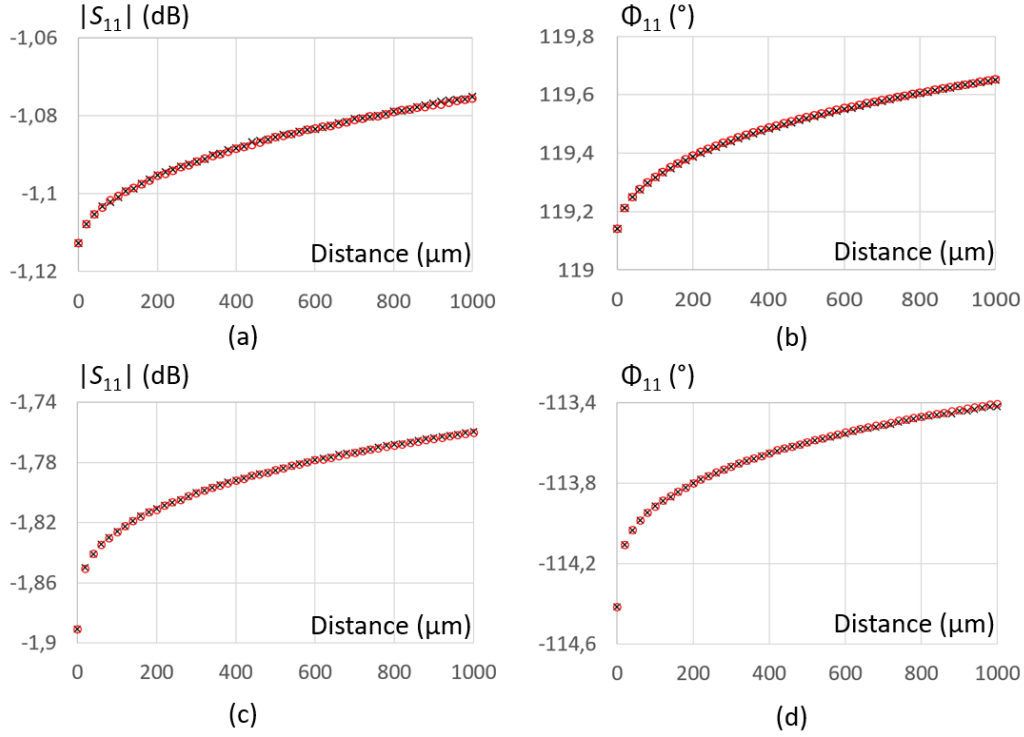


Figure 3. Amplitude and phase-shift of the reflection coefficient S_{11} as a function of the probe-metallic sample separation. (a)-(b) $f = 1 \text{ GHz}$ and (c)-(d) $f = 2 \text{ GHz}$.

Figure 3 demonstrates that measured data are highly reproducible. To appreciate the deviations between measurement data obtained in approach and retract curves respectively, statistical errors including maximum and median errors are computed for both amplitude and phase-shift of the complex reflection coefficient.

	$ S_{11} $ (dB)		Φ_{11} (°)	
	Maximum	Mean or Percentage	Maximum	Mean or Percentage
1 GHz	1.156E-3	3.720E-4 or 0.0346 %	8.662E-3	4.189E-3 or 0.00350 %
2 GHz	2.903E-3	4.246E-4 or 0.0227 %	3.031E-2	7.417E-3 or 0.00654 %

Table 2. Reproducibility errors computed on measured complex reflection coefficients S_{11} .

When the probe is moved closer to the sample, the amplitude and phase-shift of the complex reflection coefficient of the probe are strongly impacted. Indeed, the measured amplitude and phase-shift of the reflection coefficient S_{11} decays with the distance separation. To simplify the modelling, the data obtained are fitted with polynomial functions in equations (1) to (4). The coefficients of determination r^2 that qualify the goodness of fit is close to 1 for all cases considered.

$$(a) |S_{11}|_{dB} = -8E-19d^6 + 3E-15d^5 - 3E-12d^4 + 2E-09d^3 - 8E-07d^2 + 0.0002d - 1.1117 \quad (r^2 = 0.9991) \quad (1)$$

$$(b) \Phi_{11} = -1E-17d^6 + 4E-14d^5 - 5E-11d^4 + 3E-08d^3 - 1E-05d^2 + 0.0025d + 119.16 \quad (r^2 = 0.9987) \quad (2)$$

$$(c) \quad |S_{11}|_{dB} = -9E-15d^6 + 9E-12d^5 - 3E-09d^4 + 6E-07d^3 - 6E-05d^2 + 0.0028d - 1.89 \quad (r^2 = 0.9976) \quad (3)$$

$$(d) \quad \Phi_{11} = -1E-14d^6 + 1E-11d^5 - 7E-09d^4 + 2E-06d^3 - 0,0003d^2 + 0.0172d - 114.41 \quad (r^2 = 0.9936) \quad (4)$$

The d^1 -terms provides information related to the electrical sensitivity at the 1st order. In particular, amplitude sensitivities of 0.0002dB/ μm and 0.0028dB/ μm are obtained at 1GHz and 2GHz respectively. In the same manner, phase-shift sensitivities of 0.0025°/ μm and 0.0172°/ μm are determined at 1GHz and 2GHz respectively. Consequently, the electrical amplitude and phase-shift sensitivities are increased by 14 and 6.9 respectively when the operating frequency is doubled. Indeed, the measured complex reflection coefficients are function of the coupling capacitance between the metallic target and the probe tip. Whereas the phase-shift Φ_{11} of the complex reflection coefficient at the probe tip changes theoretically as a function of d , the theoretical amplitude $|S_{11}|$ should be less perturbed (radiation losses). Consequently, a calibration procedure that relates the measured complex reflection coefficient as a function of the coupling capacitance can be used to determine the calibrated complex reflection at the probe tip interface [16].

4 Application to microwave sensing of liquid droplets

In the proposed application, liquid droplets are investigated. A non-deionized water droplet is placed on the metallic sample holder. We measure the magnitude and phase shift of the reflection coefficient S_{11} at 1 GHz by varying the distance probe – liquid until a penetration of around 400 μm inside the droplet (Figure 4).

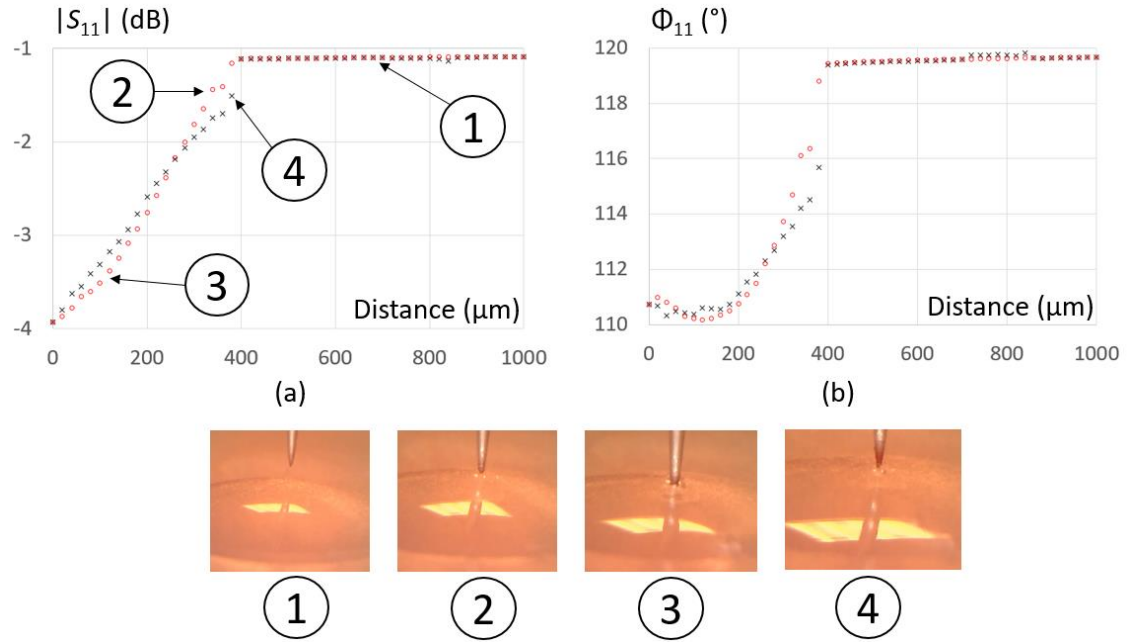


Figure 4. Measured (a) amplitude and (b) phase-shift of the complex reflection coefficients as a function of the distance (non-deionized water) at 1 GHz.

We observe a coefficient reflection / complex impedance *breakdown* at the liquid contact (step 2). A relative good variation of the reflection coefficient amplitude and phase shift is noticed for the probe displacement in the liquid ($\Delta|S_{11}| = 3 \text{ dB}$ et $\Delta\Phi_{11} = 10^\circ$). During the retract phase, the appearance of a water meniscus between the liquid and the apex of the probe impacts the measured signature (step 4). During the experiment, an electrolysis phenomenon between the sample holder (aluminum plate) and the tungsten needle through the liquid has been observed. The use of a metallic holder simplifies the modeling and dedicated calibration procedure ($S_{11} = -1$). Nevertheless, to avoid the apparition of air bubbles related to chemical reactions, we have also considered a sample holder made of a dielectric material with known dielectric properties (epoxy thickness = 1.15mm and $\epsilon_r = 4.15$). Using the same measurement configuration, we observed the probe tip inside the liquid using a camera that demonstrates stable measurements (Figure 5).

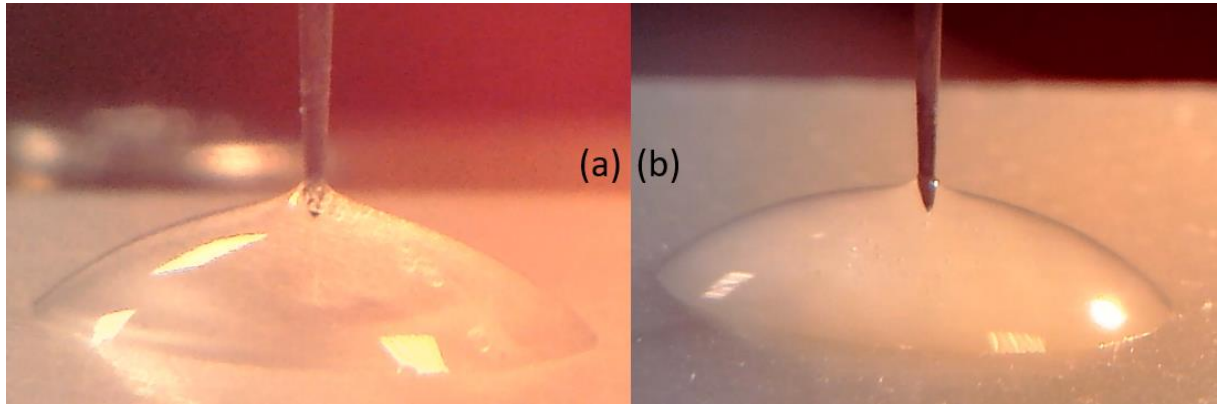


Figure 5. Photographs of the probe tip inside non deionized water during microwave radiation at 1 GHz. The liquid droplet is placed on (a) Aluminum holder (b) dielectric (Epoxy) holder.

5 Conclusion

A Microwave dielectric characterization platform dedicated to small volume of liquids has been presented. In particular, the use of an evanescent probe, showing an improved spatial resolution coupled with a nano-positioning system is a viable solution to address local and quantitative dielectric characterizations of liquids or biological materials. The preliminary tests related to water droplet performed at 1GHz and 2 GHz have demonstrated repeatable measurements considering an approach-retract scenario. Future works will include a parametric study considering different apex sizes, broadband frequency investigation, XY dielectric imaging and development of dedicated modelling for local extraction of the complex permittivity.

References

- [1] K. Haddadi, "Mesure hyperfréquence des propriétés électromagnétiques de matériaux : 300 MHz à 300 GHz" Article de référence R117v1, *Techniques de l'Ingénieur*, Déc. 2016.
- [2] T. W. Athey, M. A. Stuchly and S. S. Stuchly, "Measurement of Radio Frequency Permittivity of Biological Tissues with an Open-Ended Coaxial Line: Part I," in *IEEE Transactions on Microwave Theory and Techniques*, vol. 30, no. 1, pp. 82-86, Jan. 1982, doi: 10.1109/TMTT.1982.1131021
- [3] Y. -. Wei and S. Sridhar, "Radiation-corrected open-ended coax line technique for dielectric measurements of liquids up to 20 GHz," in *IEEE Transactions on Microwave Theory and Techniques*, vol. 39, no. 3, pp. 526-531, March 1991, doi: 10.1109/22.75296.
- [4] A. Nyshadham, C. L. Sibbald and S. S. Stuchly, "Permittivity measurements using open-ended sensors and reference liquid calibration-an uncertainty analysis," in *IEEE Transactions on Microwave Theory and Techniques*, vol. 40, no. 2, pp. 305-314, Feb. 1992
- [5] F. M. Ghannouchi and R. G. Bosisio, "Measurement of microwave permittivity using a six-port reflectometer with an open-ended coaxial line," in *IEEE Transactions on Instrumentation and Measurement*, vol. 38, no. 2, pp. 505-508, April 1989, doi: 10.1109/19.192335.
- [6] K. Haddadi and T. Lasri, "Interferometric technique for microwave measurement of high impedances," *2012 IEEE/MTT-S International Microwave Symposium Digest*, 2012, pp. 1-3, doi: 10.1109/MWSYM.2012.6259554.
- [7] H. Bakli, and K. Haddadi, "Microwave interferometry based on open-ended coaxial technique for high sensitivity liquid sensing," *Advanced Electromagnetics*, vol. 6, no. 3, pp.88-93, 2017.
- [8] H. Bakli and K. Haddadi, "Quantitative determination of small dielectric and loss tangent contrasts in liquids," *2017 IEEE International Instrumentation and Measurement Technology Conference (I2MTC)*, 2017, pp. 1-6, doi: 10.1109/I2MTC.2017.7969796.
- [9] "Keysight 85070E, Dielectric Probe Kit 200 MHz to 50 GHz," *Technical Overview*, 2017.
- [10] H. Bakli, K. Haddadi and T. Lasri, "Interferometric technique for scanning near-field microwave microscopy applications," *2013 IEEE International Instrumentation and Measurement Technology Conference (I2MTC)*, 2013, pp. 1694-1698, doi: 10.1109/I2MTC.2013.6555703.

- [11] S. Gu, K. Haddadi and T. Lasri, "Near-field microwave microscopy for liquid characterization," *2014 44th European Microwave Conference*, 2014, pp. 628-631, doi: 10.1109/EuMC.2014.6986512.
- [12] R. Dandan, Z. Nemati, C.-H. Lee, J. Li, K. Haddadi, D. C. Wallace, and P. J. Burke. "An ultra-high bandwidth nano-electronic interface to the interior of living cells with integrated fluorescence readout of metabolic activity," *in Scientific reports*, vol. 10, no. 1, pp 1-12, 2020.
- [13] M. Farina, A. Di Donato, D. Mencarelli, G. Venanzoni and A. Morini, "High Resolution Scanning Microwave Microscopy for Applications in Liquid Environment," *in IEEE Microwave and Wireless Components Letters*, vol. 22, no. 11, pp. 595-597, Nov. 2012, doi: 10.1109/LMWC.2012.2225607.
- [14] SmarAct GmbH, <https://www.smaract.com/linear-stages/product/slc-2430>, SLC-2430 - Linear Piezo Stage, *Specifications Sheet*, 2022.
- [15] SmarAct GmbH, <https://www.smaract.com/linear-stages/product/slc-1730>, SLC-1730 - Linear Piezo Stage, *Specifications Sheet*, 2022.
- [16] M. Kasper, G. Gramse and F. Kienberger, "An Advanced Impedance Calibration Method for Nanoscale Microwave Imaging at Broad Frequency Range," *in IEEE Transactions on Microwave Theory and Techniques*, vol. 65, no. 7, pp. 2418-2424, July 2017, doi: 10.1109/TMTT.2017.2661260.